

Cancer Stem Cells Are Enriched in the Side Population Cells in a Mouse Model of Glioma

Molly A. Harris,^{1,2} Hyuna Yang,¹ Benjamin E. Low,¹ Joydeep Mukherje,³ Abhijit Guha,³ Roderick T. Bronson,⁴ Leonard D. Shultz,¹ Mark A. Israel,⁵ and Kyuson Yun¹

¹The Jackson Laboratory, Bar Harbor, Maine; ²The Graduate School of Biomedical Sciences, University of Maine, Orono, Maine; ³The Hospital for Sick Children, University of Toronto, Toronto, Ontario, Canada; ⁴Harvard Medical School, Department of Pathology, Boston, Massachusetts; and ⁵Norris Cotton Cancer Center, Dartmouth-Hitchcock Medical Center, Lebanon, New Hampshire

Abstract

The recent identification of cancer stem cells (CSCs) in multiple human cancers provides a new inroad to understanding tumorigenesis at the cellular level. CSCs are defined by their characteristics of self-renewal, multipotentiality, and tumor initiation upon transplantation. By testing for these defining characteristics, we provide evidence for the existence of CSCs in a transgenic mouse model of glioma, *S100 β -verbB;Trp53*. In this glioma model, CSCs are enriched in the side population (SP) cells. These SP cells have enhanced tumor-initiating capacity, self-renewal, and multipotentiality compared with non-SP cells from the same tumors. Furthermore, gene expression analysis comparing fluorescence-activated cell sorting–sorted cancer SP cells to non-SP cancer cells and normal neural SP cells identified 45 candidate genes that are differentially expressed in glioma stem cells. We validated the expression of two genes from this list (*S100a4* and *S100a6*) in primary mouse gliomas and human glioma samples. Analyses of xenografted human glioblastoma multiforme cell lines and primary human glioma tissues show that *S100A4* and *S100A6* are expressed in a small subset of cancer cells and that their abundance is positively correlated to tumor grade. In conclusion, this study shows that CSCs exist in a mouse glioma model, suggesting that this model can be used to study the molecular and cellular characteristics of CSCs *in vivo* and to further test the CSC hypothesis. [Cancer Res 2008;68(24):10051–9]

Introduction

The fundamental basis for the cancer stem cell (CSC) hypothesis is the concept that there is a hierarchical organization of cells within a tumor and that only a subset of these cancer cells has the characteristics of stem cells (self-renewal and multipotentiality; refs. 1, 2) and can initiate a tumor when transplanted (3). In addition, CSCs are thought to contribute to metastasis, therapy resistance, and recurrence (4). Emerging studies show that CSCs are indeed more resistant to therapy than other cancer cells (5–9).

In human gliomas, early studies suggested that cancer-initiating cells are enriched in the CD133⁺ population (10). When CD133⁺ cells were injected orthotopically, as few as 100 of these cells could initiate a tumor whereas CD133[−] cells could not, even when 10,000

cells were injected (10). Furthermore, whereas CD133⁺ cells could give rise to both CD133⁺ and CD133[−] cells, CD133[−] cells could not give rise to CD133⁺ cells, indicating the more primitive differentiation status of CD133⁺ cells and the existence of cellular hierarchy in these glioma cells. However, more recent studies report that CD133[−] glioma cells can also initiate tumors and that there are tumor-initiating cells in gliomas that contain no CD133⁺ cells (11, 12). Together, these studies suggest that the CSC immunophenotype may vary among gliomas and that additional markers for CSCs are needed to better identify and study CSCs.

Whereas CSCs have been identified in many human cancers (2), including brain, breast, colon, and hematologic tumors, among others (10, 13–16), some have challenged the existence of rare cancer cells that have a unique tumor-initiating ability. For example, Strasser and colleagues have challenged the existence of CSCs, based on the fact that the current definition of CSCs relies heavily on xenografting human cancer cells into immunodeficient mice and then asking whether a specific subpopulation is endowed with the ability to initiate a tumor; this approach may select for human cancer cells that can survive in mouse microenvironment but not necessarily for differential tumor-initiating capacity (17, 18). When Strasser and colleagues (17) transplanted cells from three different murine leukemia and lymphoma models into syngeneic mice, they observed that any 10 cancer cells (unsorted) could transfer the disease, arguing that cancer-initiating cells are not rare when allogeneic transplantation is used. However, other studies have shown that there are identifiable small subpopulation of leukemic cells that are more tumorigenic than other cancer cells using another mouse model of leukemia (19). These conflicting findings underscore the need to better define and understand CSCs and to further test whether CSCs exist in mouse models of human cancer, particularly in solid tumors.

To test whether CSCs exist in mouse brain tumors, we used a transgenic mouse model of glioma in which the *S100 β* promoter drives the expression of the *verbB* gene (20). Approximately, 60% of *S100 β -verbB* mice develop “spontaneous” gliomas by 12 months of age, and on the *Trp53*^{−/−} (*p53*^{−/−}) mutant background, nearly 100% of *S100 β -verbB;p53*^{−/−} mice develop brain tumors by 4 months of age. Unlike transplanted neoplasms from xenografted human brain cancer cell lines, brain tumors in *S100 β -verbB;p53*^{−/−} mice are highly infiltrative with extensive vascularization and necrosis (ref. 20; Supplementary Fig. S1A and B). In our colony of *S100 β -verbB;p53*^{−/−} mice, most tumors observed are high-grade mixed gliomas, with histologic features observed in malignant grades III and IV human gliomas. Hence, in light of the controversy that surrounds the existence of CSCs in mouse models of human cancer, we decided to test whether this mouse model of solid tumor contains CSC-like cells. Identification

Note: Supplementary data for this article are available at Cancer Research Online (<http://cancerres.aacrjournals.org/>).

Requests for reprints: Kyuson Yun, The Jackson Laboratory, 600 Main Street, Mailbox 76, Bar Harbor, ME 04609. Phone: 207-288-6825; Fax: 207-288-6078; E-mail: Kyuson.yun@jax.org.

©2008 American Association for Cancer Research.
doi:10.1158/0008-5472.CAN-08-0786

of mouse models that contain CSCs would enable exploitation of these models to study CSCs *in vivo*, including genetic manipulations, to further test the CSC hypothesis, investigation of the influence of microenvironment on CSC behavior, large cohort studies using inbred strains of mice, and comparison of normal cells and CSCs to determine the molecular differences between these cells from the same organs.

Here, we report the existence of CSCs in a transgenic mouse brain tumor model. We show through prospective isolation and characterization of side population (SP) cells that tumor-initiating cells are enriched in the SP cells in *S100 β -verbB;p53^{-/-}* gliomas. Furthermore, SP cells show enhanced self-renewal and multipotentiality compared with non-SP cells from the same tumor, suggesting that CSCs are enriched within the SP cells. In addition, we identify a gene signature that distinguishes brain CSCs from non-stem cancer cells and normal neural stem cells (NSC). We selected two genes from this list with known expression in other aggressive human cancers (*S100A4* and *S100A6*) to test whether they are also expressed in human gliomas. Using primary human brain cancer tissues, we show that *S100A4* and *S100A6* are expressed in a subset of glioma cells. Furthermore, we show that there is a positive correlation between the glioma grade and percentages of *S100A4*-expressing and *S100A6*-expressing cells in human samples, particularly in distinguishing glioblastoma multiforme (GBM) from lower grade gliomas.

Materials and Methods

Cell cultures. Primary cells from *S100 β -verbB;p53^{-/-}* or *S100 β -verbB;p53^{+/-}* [maintained on an inbred C57BL/6J (B6) background] mouse brain tumors were isolated and cultured as tumorspheres in modified DME/F-12 supplemented with Neurocult Proliferation Supplement (Stemcell Technologies) or B27 (Invitrogen) and penicillin/streptomycin. Neurospheres were isolated from the SVZ region of C57BL6/J wild type, *Trp53^{-/-}*, and *S100 β -verbB;Trp53^{-/-}* mice and cultured in the same medium supplemented with 20 ng/mL epidermal growth factor (EGF) and 10 ng/mL basic fibroblast growth factor (bFGF). Self-renewal assays were performed by plating dissociated single cells at 1 cell/ μ L or 1 cell/10 μ L density and counting the number of spheres that formed after 6 to 7 d. Tumorspheres were induced to differentiate on poly-D-lysine/laminin-coated coverslips for 7 d using Neurocult Neural Differentiation Supplement (Stemcell Technologies; the components of this supplement are proprietary and are not available). Human brain cancer cell lines U87, SF767, and HOG were grown as monolayer cells in DMEM with 10% fetal bovine serum with penicillin/streptomycin.

Immunohistochemistry. Standard immunofluorescence/immunohistochemical protocols were used. Mice with brain tumors were perfused, and the whole brain was dissected, fixed, and embedded in OCT. Paraffin sections of human clinical GBM samples were obtained from Dr. Ab Guha (The Hospital for Sick Children), and human glioma tissue arrays were purchased from Creative Biolabs. Human glioma *S100A4⁺* and *S100A6⁺* cells xenografted into NOD.CB17-*Prkdc^{scid}/J*-immunodeficient mice were identified by immunofluorescence using an antibody against human specific nuclear antigen (HuNu, Millipore) or by establishing stable cell lines expressing green fluorescent protein before transplantation. Because HuNu double staining could not be performed on clinical specimens, we relied on cell morphology to distinguish the human cancer cells from the reactive astrocytes (Supplementary Fig. S2). The star morphology of the astrocytes was easily distinguished from the more round cancer cells. Only the rounded cells with strong immunoreactivity to *S100A4* or *S100A6* were counted. Two representative fields from each of the clinical GBM samples were counted for *S100A4⁺* and *S100A6⁺* cells and averaged. Statistical significance of *S100A4* and *S100A6* expression in different glioma grades was calculated using the Tukey test.

Average percentages of positive cells expressing differentiation markers were measured by counting positive cells from five randomly selected fields on the coverslips containing differentiated neurosphere and tumor-sphere cells.

Antibodies used for immunohistochemistry were BCRP1 (Chemicon), SOX2 (Chemicon), GFAP (Chemicon), NG2 (Chemicon), MAP2 (Chemicon), HuNu (Millipore), and *S100A6* and *S100A4* (LabVision). Fluorescent sections were imaged using a Zeiss (Axiovert 200M) microscope with Apotome and analyzed with AxioVision software or a Leica SP5 confocal microscope with 100 \times objective and a Z-stack projection.

Fluorescence-activated cell sorting analysis. Normal and tumor tissues and cultured cells were dissociated with Accutase (Invitrogen) digestion and mechanical trituration. Dissociated cells were analyzed using a standard fluorescence-activated cell sorting (FACS) protocol. Antibodies used for FACS analyses were anti-PROM1/CD133 (eBioscience and Miltenyi) and BCRP1 (Chemicon). For SP sorting, cells were incubated with Hoechst 33342 (Sigma) at a concentration of 5 μ g/mL at 37°C for 45 min. B6 bone marrow control cells were incubated for 90 min. Stained cells were rinsed and resuspended in ice-cold culture medium containing 2 μ g/mL Hoechst 33342 for FACS sorting.

Intracranial and s.c. injections. Tumor cells were injected s.c. into the flank or the brain of NOD-SCID-immunodeficient mice or C57BL/6J syngeneic mice. For intracranial injections, cells were injected using a stereotaxic device (Bregma +2.5, -1.5, -3). The animal care and use committee at Jackson Laboratory approved all animal procedures.

Real-time reverse transcription-PCR analysis. RNA was treated with DNaseI before cDNA conversion (using iScript from Bio-Rad). Real-time PCR was performed using SYBR Green Supermix (Bio-Rad) on a LightCycler PCR machine (Roche) or iQ5 PCR machine (Bio-Rad). The primers used were *S100a6*, 5'-TGAGCAAGAAGGAGCTGAAGGAGT-3' and 5'-TTCT-GATCCTTGTACGGTCCAGA-3'; *S100a4*, 5'-TTTGAGGGCTGCCAGATAAGGAA-3' and 5'-CACATGTGCGAAGAAGCCAGAGTA-3'; and *I8s*, 5'-GAGGGAGCCTGAGAAACGG-3' and 5'-GTCGGGAGTGGGTAATTTGC-3'.

Microarray data analysis. Three biological replicates of cancer 1 (3447) and cancer 2 (4346) were derived by transplanting primary tumorspheres into three recipient mice and isolating tumorsphere cells from resulting tumors. SP cells were FACS sorted from each tumorsphere line and hybridized onto separate Affymetrix GeneChips. Three neuro-SP samples were derived from three individual control mice and hybridized separately. Three non-SP samples from cancer 1 replicates were hybridized on three separate chips. Probe intensity data from 15 MOUSE430_2 Affymetrix GeneChip arrays were analyzed by R software. Affy probe was remapped by using custom CDF file (21) from Brain Array⁶ to accommodate updated genome and transcription annotation. Perfect match intensities were normalized and summarized by the robust multiarray average method. To identify differentially expressed genes between normal and cancer SP cells, cancer 1 SP versus neural SP and cancer 2 SP versus neural SP were compared. In both comparisons, *F*s statistics, a modified *F* statistics with a shrinkage estimate of variance estimation, were calculated by MAANOVA (22). *P* values were derived by 1,000 permutations, and the false discovery rate (*q* value) was calculated to correct for the multiple hypothesis-testing problem. Differentially expressed genes between cancer and neural SP cells were selected by two criteria: genes having <0.05 *q* value and >2.6 (1.5 log₂) fold change in both comparisons. Biological relationships among differentially expressed genes were studied using Ingenuity Systems⁷ software. The GEO accession number for the microarray data is GSE13490.

Results

Neurospheres and tumorspheres display distinct cellular characteristics. CSCs in solid tumors have been shown to form tumorspheres, floating colonies of cells that resemble neurospheres formed by NSCs, in culture conditions that promote maintenance

⁶ <http://brainarray.mbni.med.umich.edu/Brainarray>

⁷ www.ingenuity.com

of stem cells. To identify distinguishing cellular and molecular phenotypes of tumorspheres and normal neurospheres, we isolated and characterized tumorspheres from tumor-bearing *S100 β -verbB;p53^{-/-}* mice on a C57BL/6/J (B6) background (Fig. 1A, a) and neurospheres from asymptomatic *S100 β -verbB;p53^{-/-}*, *p53^{-/-}*, and wild-type B6 control mice (Fig. 1A, b). Tumorspheres (Fig. 1A, a) grossly resembled neurospheres (Fig. 1A, b) isolated from the

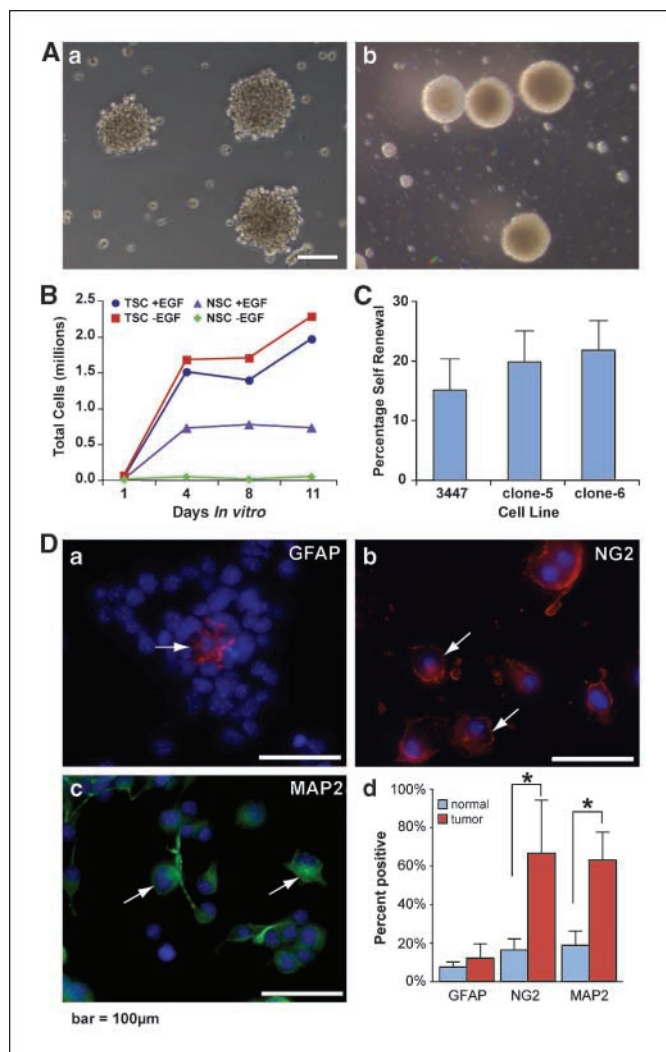


Figure 1. Isolation and characterization of tumorspheres from *S100 β -verbB;p53^{-/-}* gliomas. **A, a**, tumorspheres from *S100 β -verbB;p53^{-/-}* gliomas grown in serum-free medium without added growth factors. **b**, neurospheres isolated from the subventricular zone of asymptomatic *S100 β -verbB;p53^{-/-}* mice, grown in serum-free medium containing bFGF and EGF. **B**, growth curve comparing neurospheres and tumorspheres grown in the presence or absence of EGF (plated 1E5 cells on day 0). **C**, self-renewal assay of a parental (3447) and two clonally derived tumorsphere cell lines (measured as percentage of single cells giving rise to secondary spheres when plated at 1 cell/ μ L). **D**, dissociated tumorsphere cells plated on poly-D-lysine/laminin-coated coverslips, after 7 d in differentiation medium, stained with the following: **a**, GFAP (astrocyte marker in red; $14.1 \pm 7.33\%$); **b**, NG2 (early oligodendrocyte marker in red; $70.6 \pm 27.6\%$); **c**, MAP2 (neuronal marker in green; $66.3 \pm 14.42\%$). Arrows, positively stained cells. All nuclei are marked in blue by 4',6-diamidino-2-phenylindole (DAPI) staining. **d**, quantitation of cells expressing differentiation markers are compared between neurospheres (shown in Supplementary Fig. S3) and tumorspheres. Five fields on each coverslip were randomly selected, and positive and total cells were counted. Normal, neurosphere cells from wild-type C57BL6/J; tumor, tumorsphere cells from a *S100 β -verbB;p53^{-/-}* mouse. Asterisks, statistically significant differences calculated using the Welsh two-sample *t* test. Scale bar, 100 μ m.

subventricular zone of asymptomatic *S100 β -verbB;p53^{-/-}*, *p53^{-/-}*, and wild-type B6 mice, as well as previously described CSC-containing tumorspheres isolated from human tumors (23–25). However, tumorspheres and neurospheres showed three distinguishable cellular characteristics: (a) neurospheres absolutely required EGF for growth, whereas tumorsphere cells grew in the absence of added growth factors or serum, demonstrating growth factor independence (Fig. 1B); (b) neurospheres were round, even-edged spheres, whereas tumorspheres were more loosely attached, exhibiting an uneven periphery, indicating reduced adherence (Fig. 1A, a and b); (c) neurosphere cells never initiated tumors when injected into immunodeficient or syngeneic mice whereas most tumorspheres formed tumors (Supplementary Table S1; $P < 0.0001$).

Self-renewal, multipotentiality, and tumor-initiation of tumorspheres. To test for the frequency of tumorsphere-forming cells (cells with the ability to form floating colonies), we assessed the number of tumorspheres that form from freshly dissociated gliomas using a limiting dilution assay *in vitro*. Freshly dissociated glioma cells were plated at different doses, and the number of spheres that form after 7 days in culture was measured. The frequency of tumorsphere-forming cells ranged between 1:333 and 1:500 cells in two independent tumors tested (Supplementary Table S2), suggesting that only a small subpopulation of tumor cells from *S100 β -verbB;p53* glioma could proliferate extensively to form colonies *in vitro*. To test whether these tumorspheres contained CSCs, we tested for three defining characteristics of CSCs: self-renewal, multipotentiality, and tumor-initiating capacity.

To test for self-renewal in these tumorsphere cultures, we dissociated established tumorspheres into single cells, plated them at a clonal density (1 cell/ μ L), and counted the number of secondary spheres that formed after 7 days. Approximately, 15% to 20% of the tumorsphere cells gave rise to secondary spheres (Fig. 1C), indicating that the tumorspheres contain self-renewing stem cells. This capacity for self-renewal was maintained for >25 passages *in vitro*. To further test for the presence of stem cells, we isolated single cells and showed that they can self-renew and expand clonogenically in the absence of growth factors *in vitro* (Fig. 1C).

To test multipotentiality, tumorsphere cells were cultured in an NSC differentiation medium. Tumorsphere cells gave rise to cells expressing markers of all neural lineages, i.e., NG2⁺ (oligodendrocytes), GFAP⁺ (astrocytes), or MAP2⁺ (neurons), demonstrating multipotentiality (Fig. 1D). The frequency of GFAP⁺ cells from tumorspheres (12.2%) was similar to that from neurospheres (7.6%; $P = 0.139$). However, a significantly larger number of tumor cells expressed NG2 (66.7%) and MAP2 (63.2%) than did wild-type C57BL6/J neurosphere cells (16.3% and 18.9%, respectively; $P = 0.0112$ and 0.0005 ; Supplementary Fig. S3) after 7 days in differentiation medium. This dysregulated differentiation gene expression pattern is consistent with abnormal differentiation in cancer cells (Fig. 1D, d). Importantly, we observed identical cellular phenotypes (self-renewal and multipotentiality) in clonally derived cell lines from single tumor cells (Fig. 1C; Supplementary Table S1; data not shown).

To test tumor-initiating capacity, tumorsphere cells isolated from five independent tumors were injected either s.c. or orthotopically into the brain of either NOD.CB17-*Prkdc*^{scid}/J (NOD-SCID)-immunodeficient mice or B6 syngeneic mice (Supplementary Table S1). In all cases, the transplanted neoplasms replicated the original tumor (Supplementary Fig. S1A and B). Even

injections of individual tumorspheres (containing ~100–200 cells) formed tumors in most cases, indicating that each tumorsphere contained at least one cancer-initiating cell (Supplementary Table S1). Histologic analysis and molecular marker expression showed similar expression patterns between primary and transplanted secondary tumors in either the flank or the brain (Supplementary Fig. S1A and B). These tumors could be serially transferred through mice for more than six passages, demonstrating *in vivo* self-renewal ability. At each passage, tumorspheres were isolated and characterized, and their cellular characteristics, with respect to growth rate and marker gene expression, were similar to those of the original tumorsphere (not shown).

CSCs are enriched in the SP cells. To prospectively isolate CSCs, we examined expression patterns of candidate stem cell markers, including PROM1/CD133, BCRP1/ABCG2, CD44, c-Kit, and SOX2 in S100 β -verbB;p53 gliomas. SOX2 was expressed in the majority of cancer cells (Supplementary Fig. S1B, b–d) suggesting that this is not a unique marker for the CSC subpopulation because only a small fraction of the primary tumor cells could form tumorspheres (see above; Supplementary Table S2). This is in contrast to the normal brain of B6 mice, wherein a high-level SOX2 expression is restricted to the ependymal and subventricular zone where normal NSCs are found, with a lower level of expression in scattered cells throughout the brain (Supplementary Fig. S1B, a). ABCG2/BCRP1 was expressed in 2% to 5% of both the normal and tumorsphere cells (Supplementary Fig. S1C, a and b), and we observed weak but consistent expression of CD133 in ~0.4% to 7% of tumorsphere cells, in contrast to the expression of CD133 in ~6% to 36% of untransformed neurosphere cells (Supplementary Fig. S1C, c and d). Interestingly, CD44 and c-Kit, stem cell markers in other tissues, were expressed in 60% to 80% of cells in both tumorsphere and neurosphere cultures (not shown), consistent with the report that CD44 is a marker of glial progenitors rather than stem cells (26). None of these markers were useful in prospective isolation of CSCs in our cultures (not shown).

We then turned to another common characteristic of CSCs: the ability to extrude chemicals through the function of multidrug resistance proteins (9). Others have shown that the SP is a cellular phenotype that arises from stem cells that extrude Hoechst 33342 dye; hence, most stem cells stain only weakly with this dye. This staining method has been used by many laboratories to isolate normal and CSCs from multiple tissue types (27–30). We stained S100 β verbB;p53 tumorsphere cells with Hoechst 33342 dye and FACS sorted them for the SP and non-SP (Fig. 2A, b). We then injected SP (0.15–1.2% of viable cells) and non-SP cells from the same tumorsphere cultures into NOD-SCID mice and compared their tumor-initiating abilities. As few as 50 SP cells initiated rapid tumor growth after transplantation in host mice, whereas 500 non-SP cells were required to give rise to tumors with a similar frequency (Fig. 2B, a; Supplementary Table S3; $P = 0.0285$). This suggests that tumor-initiating cells are enriched in SP.

To test whether SP cells also show other characteristics of CSCs, we examined their self-renewal ability and multipotentiality. We sorted SP and non-SP cells and cultured them at a clonal density. SP cells consistently gave rise to a larger number of secondary spheres than did non-SP cells (Fig. 2B, b), indicating enhanced self-renewal of SP cells. In addition, we tested whether SP cells could give rise to both SP and non-SP cells, as would be expected of a stem cell population. When SP and non-SP cells were sorted and

cultured, the sorted SP cells gave rise to ~12-fold more SP cells than did the sorted non-SP cells (Fig. 2A, c and d; $P = 0.045$), consistent with a cellular hierarchy in which SP cells give rise to both SP and non-SP cells whereas non-SP cells do not (or rarely do). In addition, we consistently observed that secondary tumors contain SP⁺ cells (not shown), demonstrating *in vivo* self-renewal of SP cells. Together, these data indicate that CSCs are enriched in the SP cells in this cancer model and that SP cells can be used to examine the gene expression pattern of CSCs.

Gene expression analysis. Analysis of the molecular differences between CSCs, NSCs, and non-stem cancer cells may reveal novel markers for CSCs, as well as molecular pathways that regulate CSCs. One of the major advantages of using inbred strains of mice is the nearly identical genetic background of the different individuals of any given strain, which greatly facilitates comparative transcriptome analysis. To identify gene expression patterns

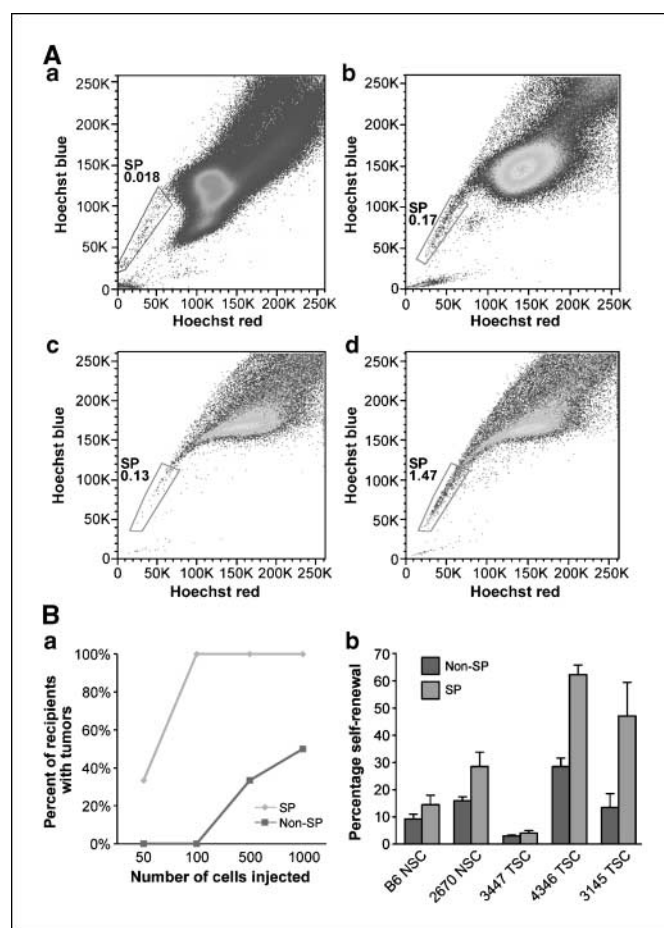


Figure 2. Isolation and characterization of cancer SP cells. **A**, Hoechst 33342 staining of bone marrow control cells (**a**) and tumorsphere cells (**b**) showing SP cells in gated areas. Tumor cells were sorted into SP and non-SP cells and cultured. Non-SP cells give rise to 0.13% SP cells (**c**) whereas SP cells give rise to 1.47% (~12-fold more) SP cells (**b**) after two passages in culture. Hoechst staining and FACS-sorted scans were performed on three independent primary tumorsphere lines with similar results ($P = 0.045$, paired *t* test). **B**, **a**, percentage of recipient mice giving rise to tumors. Graph is a summary of four independent FACS sorts and injections comparing SP and non-SP ($P = 0.0285$, logistic regression was used for statistical analysis). Two to 12 mice were injected with each cell dose (see Supplementary Table S3 for details). **b**, self-renewal assay of two neurosphere lines and three tumorsphere lines, comparing the percentages of secondary sphere formation by SP and non-SP cells ($P = 0.0471$, paired *t* test).

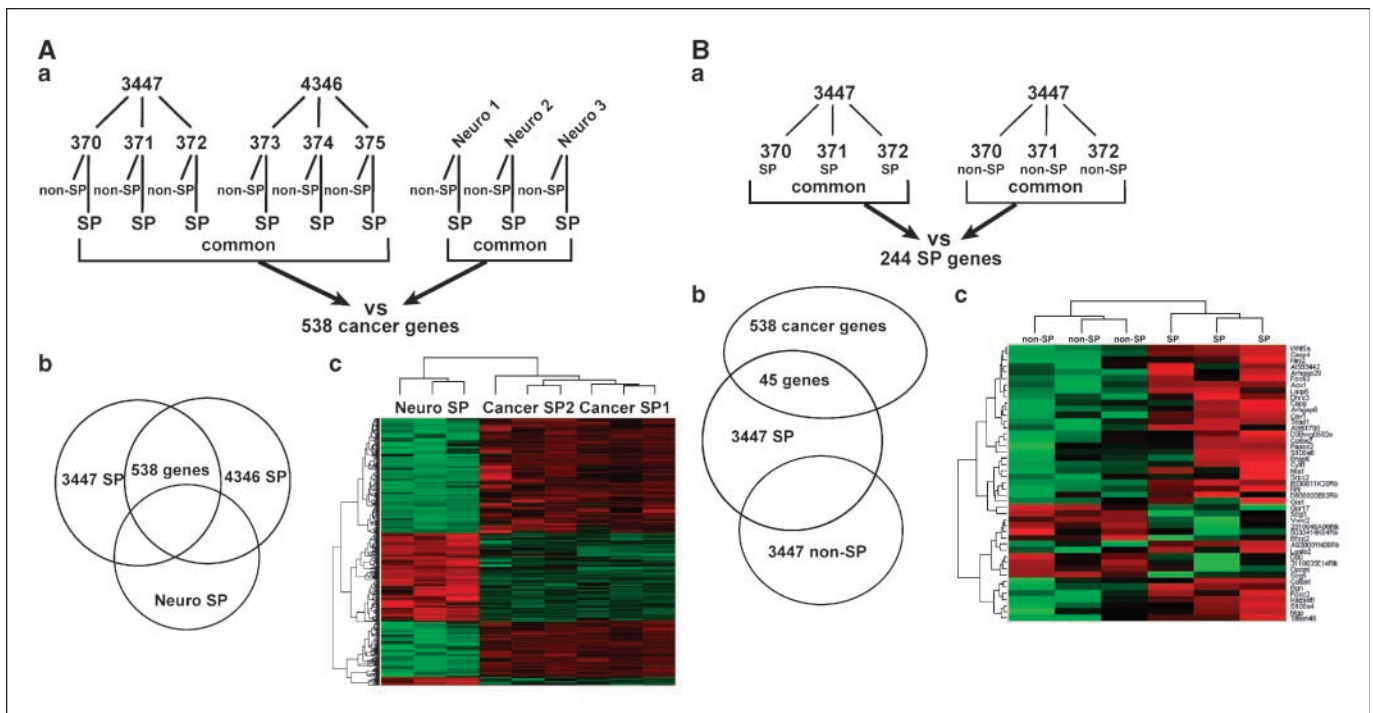


Figure 3. Microarray analysis of SP-sorted normal and cancer cells. **A, a**, SP cells were purified from six tumorsphere cultures (biological triplicates derived from transplanting two independent primary tumors) and three independent neurosphere cultures from two *p53*^{-/-} mice and one *S100 β -verbB;p53*^{-/-} mouse. **b**, 538 differentially expressed genes were identified by comparing six cancer SP and three neural SP cells with *q* value of <0.05 and log₂ change of >1.5 (cancer genes). **c**, unsupervised clustering of the 538 genes segregates cancer SP and neural SP samples. **B, a**, gene expression comparison between cancer SP and non-SP cells from the same tumor identified 244 SP genes with at least a 2-fold change in expression levels. **b**, the SP gene list was compared with the cancer gene list to identify a common subset of genes. **c**, the resulting common gene list consists of 45 genes (see Table 1), which segregates SP and non-SP samples when unsupervised clustering analysis was used. *Red*, higher level of expression in the heat-maps in (A, c) and (B, c).

that distinguish CSCs from NSCs, SP cells were isolated from both neurospheres (derived from *S100 β -verbB;p53*^{-/-} and *p53*^{-/-} brain) and tumorspheres (derived from *S100 β -verbB;p53*^{-/-} gliomas). We used neurospheres from *p53*^{-/-} background rather than wild-type B6 mice in this comparison because we wanted to identify genes that are differentially expressed in transformed cells from *S100 β -verbB;p53*^{-/-} genotype and not just downstream targets of p53. Neurosphere cells from *S100 β -verbB;p53*^{-/-} and *p53*^{-/-} mice were tested both *in vitro* and *in vivo* to ensure that they were not transformed cells (i.e., that they were growth factor-dependent and nontumorigenic) at the time of the microarray experiment (Fig. 1B; Supplementary Table S1). SP and non-SP cells were directly sorted into a lysis buffer, and labeled probes were prepared from cDNAs and hybridized onto MOUSE430_2 Affymetrix GeneChip arrays. We found that 538 genes showed consistent expression differences between the six cancer SP (biological replicates from two independent tumors) and three independent neural SP cells (*q* < 0.05 and log₂ change > 1.5; Fig. 3A). Of these, 345 genes were overexpressed and 193 genes were underexpressed in cancer-derived SP cells compared with neural SP cells (Supplementary Table S4). Unsupervised clustering of the data set using the 538 genes clearly segregated the cancer SP cells and neural SP cells (Fig. 3A, c), as expected. Real-time reverse transcription-PCR (RT-PCR) validation with selected genes showed significant expression level changes in components of the Wnt and Notch signaling pathways (*Dkk3*, *Wif1*, *Fzdb*, *Wnt7a*, *Wnt5a*, and *Hey2*), suggesting deregulation of these pathways that regulate NSCs in CSCs (Supplementary Table S5 and not shown).

To further filter the gene list for stem cell-relevant genes, we examined genes that are differentially expressed between cancer-initiating (SP) and noninitiating (non-SP) cells from the same tumorsphere cultures (Fig. 3B, a). We first identified 244 genes that showed greater than a 2-fold change in expression levels between cancer SP versus cancer non-SP cells. This list included *Nanog* and *Myc* genes associated with stem cells, validating our approach. To identify a gene list associated with glioma stem cells, we compared the two gene lists (cancer SP versus neural SP and cancer SP versus cancer non-SP cells). Forty-five genes were common to both gene lists (Fig. 3B, b). We refer to this list of 45 genes as the brain CSC signature genes, as their expression patterns distinguish cancer SP cells from untransformed neural SP and non-SP cancer cells. An unsupervised clustering analysis using this 45-gene list segregated cancer SP and non-SP samples (Fig. 3B, c).

The 45-gene list (Table 1) includes many genes with known function in cancer, such as *Bgn*, *Mgp*, *Foxc2*, *Mia1*, *Cav1*, *S100a4*, and *S100a6*. We were particularly intrigued by the expression of *Foxc2*, *S100a4/Metastasin*, and *S100a6/Calcylin* Ca⁺ binding proteins because they have been shown to mediate metastasis in other solid tumors (31–33). We chose to further examine the expression of *S100a4* and *S100a6* in CSCs by RT-PCR and immunohistochemistry. Using quantitative RT-PCR from seven independent tumorspheres, we confirmed a higher level of *S100a6* in tumorspheres compared with untransformed *S100 β -verbB;p53*^{+/-} neurospheres (Fig. 4A; *P* = 0.0019). We observed a similar pattern with *S100a4* (not shown). In addition, RNA was extracted from SP and non-SP cells from two independent tumorspheres, and the relative expression levels of *S100a6*

Table 1. 45-brain CSC signature genes

Category	N = 45	Genes
Extracellular	9	Mgp (99.5×), Bgn (102×), Kazald1 (19×), Col6a1 (15.7×), Scg5 (8.5×), Col6a2 (14.6×), Vwc2 (4.2×), Mia1 (5.9×), Scg3 (0.2×)
Membrane/cell signaling	12	Tmem46 (6.5×), Opcml (6.2×), Ninj2 (8.5×), Enpp6 (6.3×), Cav1 (15.7×), S100a6 (31.5×), S100a4 (14.7×), Gpr17 (8.7×), D930020E02Rik (0.1×), Gja1 (0.1×), 5033414K04Rik (0.2×), Kcna4 (12.9×)
Secreted	3	Cytl1 (16.1×), Al851790 (0.2×), Wnt5a (0.2×)
DNA/RNA binding	5	Foxc2 (32.6×), Foxa3 (10.6×), A930001N09Rik (4.5×), Larp6 (5.4×), Tead1 (0.3×)
Kinase/phosphatase/GTPase	4	Papss2 (39.7×), Arhgap6 (13.2), D3Bwg0562e (6.2×), Arhgap29 (0.3×)
Apoptosis	1	Casp4 (12.4×)
Novel genes	4	3110035E14Rik (12.1×), 2310046A06Rik (8.2×), E030011K20Rik (5×), Ai593442 (0.1×)
Others	7	Ddc (20.4×), Lgals2 (11.7×), Capg (15×), Srpx2 (7.4×), Dhrr3 (4.1×), Bfsp2 (15.1×), Aox1 (0.3×)

NOTE: Average fold change between normal SP and cancer SP from the microarray analysis are indicated in parentheses. Selected genes were validated with RT-PCR (in bold).

and *S100a4* were measured by quantitative RT-PCR. Confirming our microarray results, both *S100a6* and *S100a4* were expressed higher in cancer SP cells than in non-SP cells from the same tumors (Fig. 4B). Finally, on primary *S100β-verbB;p53* glioma sections, only a small subset (2–4%) of cells expressed S100A4 and S100A6 proteins, consistent with their potential expression in CSCs (Fig. 4C). Together, these results suggest that *S100a6* and *S100a4* are candidate markers for CSCs in gliomas.

S100A4 and S100A6 expression in human gliomas. To test whether *S100A4* and *S100A6* are expressed in human gliomas, we examined the expression patterns of S100A4 and S100A6 in clinical GBM samples, human brain tumor tissue arrays, and tumors derived from intracranial xenografts of human brain cancer cell lines (U87, SF767, and HOG cells) into NOD-SCID mice. In xenografted tumors, a subset of S100A4⁺ and S100A6⁺ cells coexpressed human-specific nuclear antigen (HuNu; Fig. 5A, a and b), indicating that these are transplanted cancer cells. These S100A4-expressing and S100A6-expressing cells were often positioned in the periphery of the tumor or adjacent to blood vessels (not shown), the latter of which is a proposed niche for NSCs and glioma CSCs (34, 35). In clinical samples, strong S100A6 and S100A4 cytoplasmic staining was observed in scattered cancer cells throughout the tumors in all five GBM samples examined (Fig. 5B and C). Significantly, in all tumors examined, many S100A6⁺ and S100A4⁺ cells were often observed adjacent to blood vessels (Fig. 5B). The percentages of S100A4⁺ and S100A6⁺ cells varied among individual GBM samples (7.57–26.93%; Fig. 5C) but the percentages of S100A4⁺ and S100A6⁺ cells in each of the samples were very similar ($P = 0.88$).

It was previously proposed that the abundance of CSCs may correlate with the tumor grade (25). To examine whether *S100A4* and *S100A6* expression patterns correlate with tumor grade, we used a brain tumor tissue array containing normal

brain tissue and gliomas from grade I through grade IV. As shown in Fig. 5D, the percentages of *S100A4*-expressing cells in the different samples showed a positive correlation with tumor grade: normal tissue had no S100A4-positive cells, low-grade gliomas had very few positive cells, and grade IV glioma samples had a large number of S100A4 expressing cells (>8% of total cells). In particular, S100A4 expression could clearly distinguish grade III and grade IV gliomas ($P < 0.001$; Fig. 5D and Supplementary Fig. S2B).

Discussion

In this report, we provide evidence for the first time that CSCs exist in a mouse model of glioma, rendering support for the CSC hypothesis. We present several lines of evidence that, in the *S100β100β-verbB;p53* glioma mouse model, CSCs are enriched in SP cells. SP cells exhibit increased self-renewal ability, as shown by an increased percentage of secondary sphere formation (Fig. 2B, b) and generation of an increased number of SP cells upon culture (Fig. 2A, d). Importantly, SP cells are more tumorigenic than non-SP cells (Fig. 2B, a; Supplementary Table S3).

Whereas earlier studies suggested that CSCs are enriched in the CD133⁺ population in human gliomas, more recent studies indicate that not all glioma stem cells are CD133⁺. While we were able to show that CSCs exist in *S100β-verbB;p53* gliomas, we were not able to purify CSCs using PROM1/CD133 expression. Emerging studies are consistent with this in showing that CD133 is not an obligate marker for CSC in gliomas; some CD133⁻ cells have been shown to be tumorigenic and have the potential to give rise to CD133⁺ cells (11, 12). We do not know yet whether the *S100β-verbB;p53* model is representative of human gliomas in which CSCs are CD133⁻ or whether CD133 antibodies that are available for mouse PROM1/CD133 do not have strong affinity for the glycosylated form of CD133 present on cancer cells.

Recent studies indicate molecular heterogeneity among CSCs (11, 12, 36, 37), suggesting that a single marker is unlikely to identify all CSCs even within tumors of the same clinical grade from the same organ. We were unable to identify CSCs in *S100 β -verbB;p53* gliomas using an immunophenotype (including ABCG2/BCRP1 or CD133 expression); hence, we used a cellular phenotype common to stem cells to sort for a specific subpopulation (SP) that enriches for CSCs. Staining for SP cells has been used to isolate bone marrow stem cells for many years (38), and recently, this technique has been adopted by many researchers to enrich for normal cells and CSCs from multiple tissue types (28, 29, 39). For example, Kondo and colleagues have shown that cancer-initiating cells of the C6 rat glioma cell line are enriched in the SP (28), and others have previously shown that normal NSCs neurosphere cultures are enriched in the SP (29), consistent with our observations (Fig. 2B, b). However, some have reported increased cellular toxicity associated with Hoechst 33342 staining (a staining technique used to identify SP cells), questioning the usefulness of this technique to test for tumor initiation (40). In our hands,

we observe equivalent levels of cell death in FACS-sorted SP and non-SP cells, most likely from the sorting itself, suggesting that selective cell death is not the major reason for the differential tumorigenic potential we observe with SP cells.

Whereas the molecular heterogeneity of SP cells is unknown in this tumor model, the relative enrichment (10-fold to 20-fold) of CSCs in the SP compared with non-SP tumorsphere cells (Fig. 2B, a; Supplementary Table S3) is sufficient to enable the identification of candidate genes that are differentially expressed in CSCs. By comparing purified populations of cells enriched in cancer stem versus normal stem cells and in cancer stem versus non-stem cancer cells, we identified a small number of genes whose expression distinguishes brain CSCs from NSCs and non-stem cancer cells. Notably, 24 of the 45 genes encode either secreted or membrane proteins or extracellular matrix components (Table 1), suggesting that a major distinguishing feature of the glioma SP cells we analyzed is their ability to interact with their microenvironment. The ability of cancer cells to establish themselves in a foreign cellular environment is an essential characteristic for successful metastasis and a defining characteristic of CSCs. Consistently, many genes on our list have known functions in mediating breast cancer metastasis. For example, a recent study has shown that FOXC2, a transcription factor on the list, is important in mediating breast cancer metastasis by regulating expression of genes that are involved in epithelial-mesenchymal transition (32). Consistently, we observed higher levels of *Snai2*, a transcription factor regulated by *Foxc2*, in tumorspheres than normal neurospheres (Supplementary Table S5). In addition, *S100a4/metastasin/Fsp1* was originally cloned as a gene that is differentially expressed in metastatic breast cancer cells, and it has been shown to have a causal role in mediating breast cancer metastasis (41, 42). Expression level of other genes on the list, such as *S100A6*, has been shown to correlate with pancreatic cancer prognosis (43) and colon cancer invasion/metastasis (33, 44). These observations suggest an intriguing possibility that the same molecular pathways that regulate metastasis in neoplasms outside of the nervous system may also be involved in gliomas.

Whereas *S100A4* and *S100A6* expression and function have not been reported in some cell populations in the brain, this has not been previously reported in brain cancer cells. In rodent brains, *S100a4* was reported to be expressed in a subset of white matter glial cells and reactive astrocytes after injury (45). Whereas we do observe *S100A4*⁺/GFAP⁺ reactive astrocytes in transplant-recipient mouse brains, we were able to specifically identify *S100A4*⁺ cancer cells, as the astrocytes were distinguishable from cancer cells by their normal cellular morphology and GFAP expression (Supplementary Fig. S2A; data not shown). Similarly, *S100a6/Calcyclin* was reported to be expressed in the subventricular zone and ependymal layer of the normal brain (46), wherein *Prom1/CD133*, *Sox2*, and *Nestin* (markers of NSCs) are also expressed. In human and mouse glioma samples, we observed that (a) only a small subset of cancer cells express *S100A4* and *S100A6* (Figs. 4C and 5) and (b) many *S100A4*⁺ and *S100A6*⁺ cells are associated with the stem cell niche in the brain, the endothelium (Fig. 5B; refs. 34, 35). In support of a link between these genes and CSCs, *S100A4* and *S100A6* expression has been reported to be associated with other stem cells (47, 48). We are currently testing the hypothesis that *S100A4* and *S100A6* may be new markers for CSCs by prospective sorting and transplantation of *S100A4*⁺ or *S100A6*⁺ cells in *S100 β -verbB;p53* gliomas and by examining coexpression of *S100A4* and *S100A6* with known stem cell markers in human gliomas.

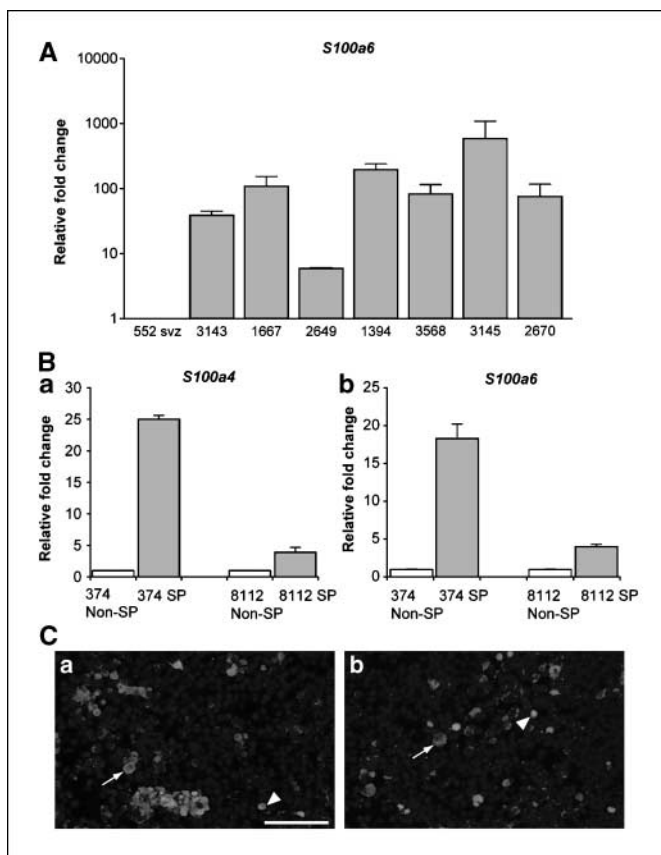


Figure 4. *S100a4* and *S100a6* expression levels are elevated in cancer SP cells. **A**, real-time RT-PCR analysis using RNA from two untransformed neurospheres from *S100 β -verbB;p53*^{-/-} mice and seven independent tumorsphere lines from *S100 β -verbB;p53*^{-/-} or *S100 β -verbB;p53*^{+/-} gliomas. Relative *S100a6* expression levels in tumorspheres are compared with the untransformed neurosphere levels ($P = 0.0019$, Welsh two-sample t test). **B**, relative *S100a4* (**a**) and *S100a6* (**b**) expression levels between SP and non-SP cells, with the non-SP level set at 1. Analyzed with two independent tumorsphere lines and repeated with at least three technical replicates. All samples in **A** and **B** were normalized to internal 18S levels. **C**, immunofluorescence analysis of primary mouse gliomas using an antibody against *S100A6* (**a**) and *S100A4* (**b**). Both cytoplasmic (arrow) and nuclear (arrowhead) staining was observed for both antibodies. All nuclei are marked in blue by DAPI staining. Scale bar, 100 μ m.

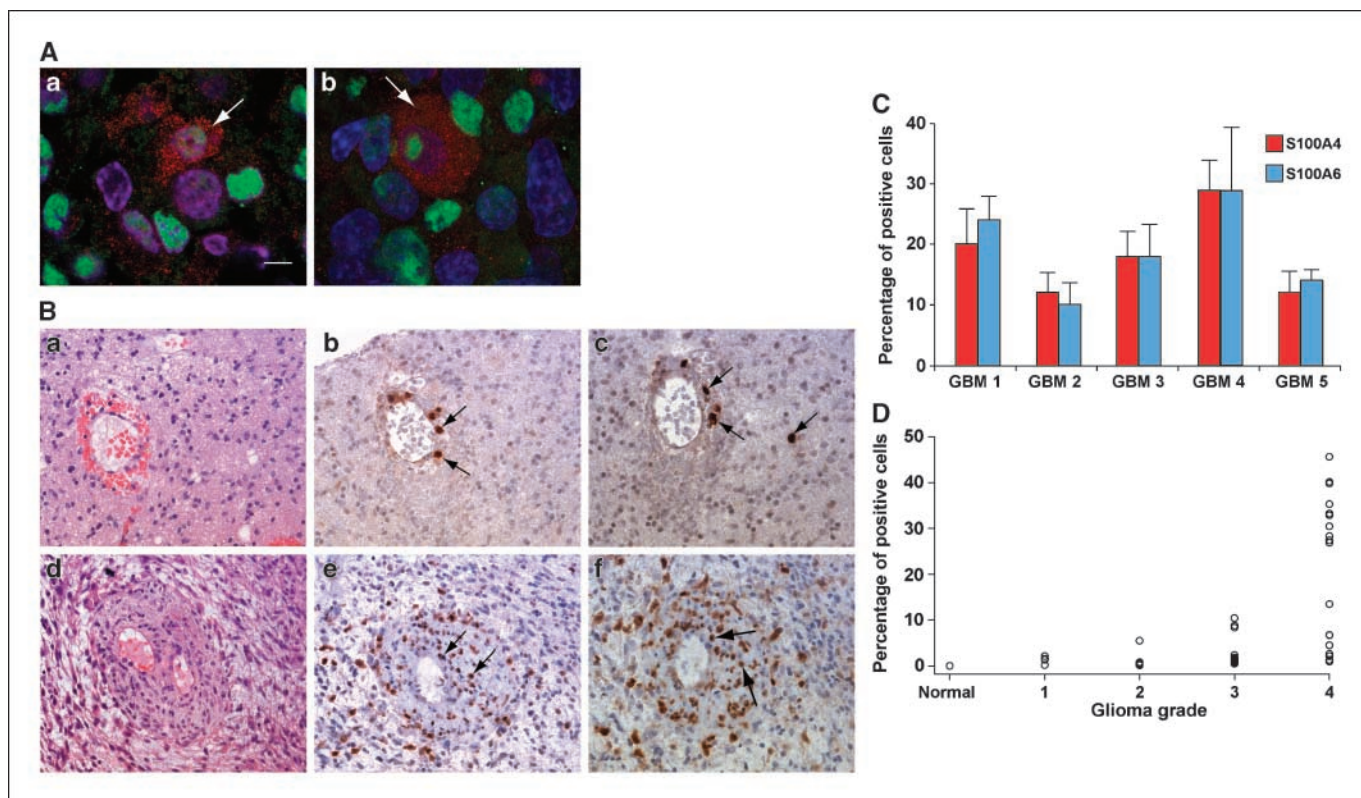


Figure 5. S100A6 and S100A4 expression in human brain tumor tissues. *A*, immunofluorescence analysis of U87 (a human GBM cell line) xenografted tumor, using an antibody against S100A4 (*a*) and S100A6 (*b*), both in red, human nuclear antigen (HuNu) antibody in green, and DAPI in blue (*a*, *b*). *B*, primary human GBM samples; *a-c*, GBM2; *d-f*, GBM4. H&E staining (*a*, *d*) and adjacent sections stained with S100A4 (*b*, *e*) and S100A6 (*c*, *f*). Arrows, S100A4⁺ or S100A6⁺ human cells. *C*, average percentage of S100A4⁺ and S100A6⁺ cells in five independent human GBM tissues ($P = 0.881$, Welsh two-sample *t* test). Averages were calculated from counts of three randomly chosen fields from each tumor. *D*, tissue arrays containing triplicates of normal cerebrum tissue and 19 independent human gliomas of varying grades were stained with S100A4 antibody. Graph represents the average percentage of S100A4⁺ cells in each sample (averaged from two random fields) from 16 tumors (five grade IV, six grade III, two grade II, and one grade I) and three normal tissue samples. Expression of S100A4 was significantly higher in grade IV compared with grade III gliomas ($P < 0.001$, Tukey test), as well as between grade IV gliomas and grade II gliomas, grade I gliomas, and normal tissue samples. Two independent neuropathologists determined the tumor grades on the tissue array using the WHO grading scheme. Scale bar, 100 μ m.

Regardless of whether S100A4 and S100A6 expression identifies human glioma stem cells, our data indicate that the abundance of S100A4⁺ and S100A6⁺ cells in clinical glioma samples distinguishes undifferentiated, aggressive GBMs (grade IV) from grade III gliomas ($P < 0.001$; Fig. 5D and not shown). Using 19 different primary human samples (triplicate plugs from each sample), we show that only grade IV GBM samples contain >8% S100A4⁺ cells. Whereas a study involving a larger sample size is needed to further validate this finding, our pilot study provides a promising indication that the genes we identified by studying mouse gliomas may be useful in studying human gliomas. Considering the significant differences in the clinical outcomes and treatment regimens for GBM patients compared with those for patients with lower grade gliomas, a retrospective and/or a prospective study involving a larger set of samples to validate the use of S100A4 and S100A6 as biomarkers for GBMs and CSCs is a promising line of investigation.

While this manuscript was in revision, another group reported the identification of a population of tumor-initiating cells in a mouse model of breast cancer (49), supporting the existence of CSC-like cells in mouse models of solid tumors. Together with other studies using mouse models (19, 50), our study provides growing support for the CSC hypothesis. Therefore, in selected tumor models, murine cancer cells are organized in a hierarchy

consistent with the CSC hypothesis and the understanding of the biology of CSCs (cell of origin, therapy resistance, and stem-niche interaction, for example) can be significantly advanced using these *in vivo* models.

Disclosure of Potential Conflicts of Interest

H. Yang and K. Yun are inventors on a patent application containing some subject matter that is described in this article; the application is assigned to The Jackson Laboratory and managed by The Jackson Laboratory office of technology transfer. The other authors disclosed no potential conflicts of interest.

Acknowledgments

Received 3/9/2008; revised 7/31/2008; accepted 8/20/2008.

Grant support: Betz Foundation grant (M.A. Israel), TJL Cancer Center Support grant CA034196, and National Brain Tumor Foundation oligodendroglioma grant (K. Yun).

The costs of publication of this article were defrayed in part by the payment of page charges. This article must therefore be hereby marked *advertisement* in accordance with 18 U.S.C. Section 1734 solely to indicate this fact.

We thank Eric Dufour, Ted Duffy, Will Schott, Sonya Kamdar, Weidong Zhang, and Karen Hammond for their assistance with this project, Kevin Mills, Shaoguang Li, Susan Ackerman, Gary Churchill, Barbara Tennent, and Barbara Knowles for critical reading of this manuscript, Jackson Laboratory's Multimedia Services for their assistance with graphic arts, and all members of the Yun laboratory for their input and help throughout this project.

References

1. Bonnet D, Dick JE. Human acute myeloid leukemia is organized as a hierarchy that originates from a primitive hematopoietic cell. *Nat Med* 1997;3:730-7.
2. Dalerba P, Cho RW, Clarke MF. Cancer stem cells: models and concepts. *Annu Rev Med* 2007;58:267-84.
3. Wicha MS, Liu S, Dontu G. Cancer stem cells: an old idea-a paradigm shift. *Cancer Res* 2006;66:1883-90; discussion 95-6.
4. Zhang M, Rosen JM. Stem cells in the etiology and treatment of cancer. *Curr Opin Genet Dev* 2006;16:60-4.
5. Ma S, Lee TK, Zheng BJ, Chan KW, Guan XY. CD133(+) HCC cancer stem cells confer chemoresistance by preferential expression of the Akt/PKB survival pathway. *Oncogene* 2007;27:1749-58.
6. Bao S, Wu Q, McLendon RE, et al. Glioma stem cells promote radioresistance by preferential activation of the DNA damage response. *Nature* 2006;444:756-60.
7. Liu G, Yuan X, Zeng Z, et al. Analysis of gene expression and chemoresistance of CD133+ cancer stem cells in glioblastoma. *Mol Cancer* 2006;5:67.
8. Rich JN. Cancer stem cells in radiation resistance. *Cancer Res* 2007;67:8980-4.
9. Dean M, Fojo T, Bates S. Tumour stem cells and drug resistance. *Nat Rev Cancer* 2005;5:275-84.
10. Singh SK, Hawkins C, Clarke ID, et al. Identification of human brain tumour initiating cells. *Nature* 2004;432:396-401.
11. Beier D, Hau P, Proescholdt M, et al. CD133(+) and CD133(-) glioblastoma-derived cancer stem cells show differential growth characteristics and molecular profiles. *Cancer Res* 2007;67:4010-5.
12. Wang J, Sakariassen PO, Tsinkalovsky O, et al. CD133 negative glioma cells form tumors in nude rats and give rise to CD133 positive cells. *Int J Cancer* 2008;122:761-8.
13. Prince ME, Sivanandan R, Kaczorowski A, et al. Identification of a subpopulation of cells with cancer stem cell properties in head and neck squamous cell carcinoma. *Proc Natl Acad Sci U S A* 2007;104:973-8.
14. O'Brien CA, Pollett A, Gallinger S, Dick JE. A human colon cancer cell capable of initiating tumour growth in immunodeficient mice. *Nature* 2007;445:106-10.
15. Al-Hajj M, Wicha MS, Benito-Hernandez A, Morrison SJ, Clarke MF. Prospective identification of tumorigenic breast cancer cells. *Proc Natl Acad Sci U S A* 2003;100:3983-8.
16. Dalerba P, Dylla SJ, Park IK, et al. Phenotypic characterization of human colorectal cancer stem cells. *Proc Natl Acad Sci U S A* 2007;104:10158-63.
17. Kelly PN, Dakic A, Adams JM, Nutt SL, Strasser A. Tumor growth need not be driven by rare cancer stem cells. *Science* 2007;317:337.
18. Hill RP. Identifying cancer stem cells in solid tumors: case not proven. *Cancer Res* 2006;66:1891-5; discussion 0.
19. Yilmaz OH, Valdez R, Theisen BK, et al. Pten dependence distinguishes haematopoietic stem cells from leukaemia-initiating cells. *Nature* 2006;441:475-82.
20. Weiss WA, Burns MJ, Hackett C, et al. Genetic determinants of malignancy in a mouse model for oligodendroglioma. *Cancer Res* 2003;63:1589-95.
21. Dai M, Wang P, Boyd AD, et al. Evolving gene/transcript definitions significantly alter the interpretation of GeneChip data. *Nucleic Acids Res* 2005;33:e175.
22. Wu H, Kerr K, Churchill GA. MAANOVA: a software package for the analysis of spotted cDNA microarray experiments. *The Analysis of Gene Expression Data: An Overview of Methods and Software* 2003:313-431.
23. Galli R, Binda E, Orfanelli U, et al. Isolation and characterization of tumorigenic, stem-like neural precursors from human glioblastoma. *Cancer Res* 2004;64:7011-21.
24. Hemmati HD, Nakano I, Lazareff JA, et al. Cancerous stem cells can arise from pediatric brain tumors. *Proc Natl Acad Sci U S A* 2003;100:15178-83.
25. Singh SK, Clarke ID, Terasaki M, et al. Identification of a cancer stem cell in human brain tumors. *Cancer Res* 2003;63:5821-8.
26. Liu Y, Han SS, Wu Y, et al. CD44 expression identifies astrocyte-restricted precursor cells. *Dev Biol* 2004;276:31-46.
27. Patrawala L, Calhoun T, Schneider-Broussard R, Zhou J, Claypool K, Tang DG. Side population is enriched in tumorigenic, stem-like cancer cells, whereas ABCG2+ and ABCG2- cancer cells are similarly tumorigenic. *Cancer Res* 2005;65:6207-19.
28. Kondo T, Setoguchi T, Taga T. Persistence of a small subpopulation of cancer stem-like cells in the C6 glioma cell line. *Proc Natl Acad Sci U S A* 2004;101:781-6.
29. Kim M, Morshead CM. Distinct populations of forebrain neural stem and progenitor cells can be isolated using side-population analysis. *J Neurosci* 2003;23:10703-9.
30. Goodell MA, McKinney-Freeman S, Camargo FD. Isolation and characterization of side population cells. *Methods Mol Biol* 2005;290:343-52.
31. Garrett SC, Varney KM, Weber DJ, Bresnick AR. S100A4, a mediator of metastasis. *J Biol Chem* 2006;281:677-80.
32. Mani SA, Yang J, Brooks M, et al. Mesenchyme forkhead 1 (FOXC2) plays a key role in metastasis and is associated with aggressive basal-like breast cancers. *Proc Natl Acad Sci U S A* 2007;104:10069-74.
33. Komatsu K, Kobune-Fujiwara Y, Andoh A, et al. Increased expression of S100A6 at the invading fronts of the primary lesion and liver metastasis in patients with colorectal adenocarcinoma. *Br J Cancer* 2000;83:769-74.
34. Calabrese C, Poppleton H, Kocak M, et al. A perivascular niche for brain tumor stem cells. *Cancer Cell* 2007;11:69-82.
35. Shen Q, Goderie SK, Jin L, et al. Endothelial cells stimulate self-renewal and expand neurogenesis of neural stem cells. *Science* 2004;304:1338-40.
36. Hermann PC, Huber SL, Herrler T, et al. Distinct populations of cancer stem cells determine tumor growth and metastatic activity in human pancreatic cancer. *Cell Stem Cell* 2007;1:313-23.
37. le Viseur C, Hofli M, Bomken S, et al. In childhood acute lymphoblastic leukemia, blasts at different stages of immunophenotypic maturation have stem cell properties. *Cancer Cell* 2008;14:47-58.
38. Goodell MA, Brose K, Paradis G, Conner AS, Mulligan RC. Isolation and functional properties of murine hematopoietic stem cells that are replicating *in vivo*. *J Exp Med* 1996;183:1797-806.
39. Szotek PP, Pieretti-Vanmarck R, Masiakos PT, et al. Ovarian cancer side population defines cells with stem cell-like characteristics and Mullerian inhibiting substance responsiveness. *Proc Natl Acad Sci U S A* 2006;103:11154-9.
40. Siemann DW, Keng PC. Cell cycle specific toxicity of the Hoechst 33342 stain in untreated or irradiated murine tumor cells. *Cancer Res* 1986;46:3556-9.
41. Davies MP, Rudland PS, Robertson L, Parry EW, Jolicoeur P, Barraclough R. Expression of the calcium-binding protein S100A4 (p9Ka) in MMTV-neu transgenic mice induces metastasis of mammary tumours. *Oncogene* 1996;13:1631-7.
42. Grum-Schwensen B, Klingelhofer J, Berg CH, et al. Suppression of tumor development and metastasis formation in mice lacking the S100A4(mts1) gene. *Cancer Res* 2005;65:3772-80.
43. Ohuchida K, Mizumoto K, Yu J, et al. S100A6 is increased in a stepwise manner during pancreatic carcinogenesis: clinical value of expression analysis in 98 pancreatic juice samples. *Cancer Epidemiol Biomarkers Prev* 2007;16:649-54.
44. Komatsu K, Murata K, Kameyama M, et al. Expression of S100A6 and S100A4 in matched samples of human colorectal mucosa, primary colorectal adenocarcinomas and liver metastases. *Oncology* 2002;63:192-200.
45. Kozlova EN, Lukanidin E. Metastasis-associated mts1 (S100A4) protein is selectively expressed in white matter astrocytes and is up-regulated after peripheral nerve or dorsal root injury. *Glia* 1999;27:249-58.
46. Yamashita N, Ilg EC, Schafer BW, Heizmann CW, Kosaka T. Distribution of a specific calcium-binding protein of the S100 protein family, S100A6 (calcylin), in subpopulations of neurons and glial cells of the adult rat nervous system. *J Comp Neurol* 1999;404:235-57.
47. Tumber T, Guasch G, Greco V, et al. Defining the epithelial stem cell niche in skin. *Science* 2004;303:359-63.
48. Morris RJ, Liu Y, Marles L, et al. Capturing and profiling adult hair follicle stem cells. *Nat Biotechnol* 2004;22:411-7.
49. Zhang M, Behbod F, Atkinson RL, et al. Identification of tumor-initiating cells in a p53-null mouse model of breast cancer. *Cancer Res* 2008;68:4674-82.
50. Cho RW, Wang X, Diehn M, et al. Isolation and molecular characterization of cancer stem cells in MMTV-Wnt-1 murine breast tumors. *Stem Cells* 2008;26:364-71.